

H. M. Wu · J. P. Tu · X. T. Chen · Y. Li  
X. B. Zhao · G. S. Cao

## Effects of Ni-ion doping on electrochemical characteristics of spinel $\text{LiMn}_2\text{O}_4$ powders prepared by a spray-drying method

Received: 20 September 2005 / Revised: 17 October 2005 / Accepted: 9 November 2005 / Published online: 13 December 2005  
© Springer-Verlag 2005

**Abstract** Spinel  $\text{LiMn}_{2-x}\text{Ni}_x\text{O}_4$  compounds doped with a range of Ni ( $x=0\text{--}0.06$ ) were synthesized by a spray-drying method. The structure and morphology characteristics of the powders were studied in detail by means of X-ray diffraction (XRD), scanning electron microscopy, and transmission electron microscopy. The XRD data reveal that all the samples have well-defined spinel structure, but, with the increase in Ni content, the doped lithium manganese spinels have smaller lattice constant. The undoped and doped spinel  $\text{LiMn}_2\text{O}_4$  particles are fine, narrowly distributed, and well crystallized. The electrochemical characteristics of the samples are measured in the coin-type cells in a potential range of 3.2–4.35 V vs  $\text{Li}/\text{Li}^+$ . All cyclic voltammogram curves exhibit two pairs of redox reaction peaks, but, among them, there are some differences about the peak split. With the increase in the Ni content, the specific capacities of the samples decrease slightly, but their cyclic ability increases.

**Keywords**  $\text{LiMn}_2\text{O}_4$  powders · Electrochemical property · Ni-doped, Spray-drying method · Lithium ion batteries

### Introduction

Lithium ion batteries have been studied extensively for the past 20 years due to their highest specific energy. In 1990, Sony Energy Technical [1] used  $\text{LiCoO}_2$  as cathode material and graphite as anode material and developed the commercial lithium ion batteries successfully.  $\text{LiCoO}_2$ , because of its high cost and environmental toxicity of cobalt, much effort has been done to develop alternatives [2]. At present, spinel  $\text{LiMn}_2\text{O}_4$  is considered a promising

and attractive cathode material for lithium ion batteries due to its high-reduction potential, low cost, and acceptable environmental impact as compared to  $\text{LiCoO}_2$  [3–5].

Unfortunately,  $\text{LiMn}_2\text{O}_4$ , used as a cathode in lithium ion batteries, exhibits capacity fading during cycling. After many studies, the capacity fading is mainly due to the following reasons: (a) the decomposition of the electrolyte at high-voltage region, (b) the dissolution of  $\text{Mn}^{3+}$  ions into the electrolyte, and (c) the Jahn-teller distortion [6–8]. To improve the cycle performance of the spinel  $\text{LiMn}_2\text{O}_4$ , doping and coating of  $\text{LiMn}_2\text{O}_4$  were considered to be the effective methods. Several attempts have been made for synthesizing improved lithium manganese spinel doped with various elements, such as Al, Ni, Mg, Co, Cr, Nd, and so on. In these works, many methods, like solid-state reaction and soft-chemical method, have been introduced [9–14], but the solid-state reaction could not provide good control on the crystalline growth, compositional homogeneity, particles morphology, and microstructure. In addition, the usual soft-chemical method leads to the cost of expensive reagents and process complexity.

In this present work, an attempt was made for improving cycling ability of  $\text{LiMn}_2\text{O}_4$  doped with Ni. In addition, a spray-drying method is used to prepare the powders. Spray-drying method has its many advantages, including the fact that it is a simple system and its cost effectiveness, and it can be scaled up to ton quantities. Thus, the morphology, structure, and electrochemical characteristics of undoped and doped  $\text{LiMn}_2\text{O}_4$  with different Ni content prepared by spray-drying method are investigated for comparison in detail.

### Experimental

Ni-ion-doped spinel  $\text{LiMn}_2\text{O}_4$  was synthesized by a spray-drying method. Stoichiometric amounts of  $\text{CH}_3\text{COOLi} \cdot 2\text{H}_2\text{O}$  (99%),  $\text{Ni}(\text{CH}_3\text{COO})_2 \cdot 4\text{H}_2\text{O}$  (99%), and  $\text{Mn}(\text{CH}_3\text{COO})_2 \cdot 4\text{H}_2\text{O}$  (99%) were completely dissolved in distilled water at room temperature. Through the aid of a spray-dryer, the resulting solution was dried to form a mixture of

H. M. Wu · J. P. Tu (✉) · X. T. Chen · Y. Li ·

X. B. Zhao · G. S. Cao

Department of Materials Science and Engineering,  
Zhejiang University,  
Hangzhou 310027, China

e-mail: tujp@cmsce.zju.edu.cn  
Tel.: +86-571-87952573  
Fax: +86-571-87952856

precursor by first atomizing through a sprinkler at an air pressure of 0.2 MPa and then spray-drying by hot air with the inlet temperature at 220°C and the exit air temperature at 110°C. The as-prepared precursor powders were sintered at 500°C for 6 h in dry air, and then the obtained products were ground in an agate mortar and reannealed at 750°C for 24 h. In these experiments, the atom ratios were controlled at  $\text{LiMn}_{2-x}\text{Ni}_x\text{O}_4$  ( $x=0.01, 0.02, 0.04, 0.06$ ). An excess amount of  $\text{CH}_3\text{COOLi}\cdot 2\text{H}_2\text{O}$  (2 mol%) was added to compensate for the loss due to the volatilization of lithium at high temperature.

X-ray diffraction (XRD; Rigaku D/max-rA diffractometer with  $\text{Cu K}\alpha$  radiation), field emission scan electron microscopy (SEM) (FEI SIRION JY/T010-1996), and transmission electron microscope (TEM; JEM-2010) were employed to characterize the prepared powders. XRD data were obtained at  $2\theta=10^\circ\text{--}80^\circ$ .

Electrochemical performances of the as-prepared powders were investigated with a two-electrode, coin-type cell (CR 2025), with lithium foil as the reference electrode. All testing electrodes were obtained by coating the slurry of a mixture [composed of 80 wt% active powders, 10 wt% conducting agent (acetylene black), and 10 wt% binders (polyvinylidene fluoride)] onto an aluminum foil current collector (the diameter is 12 mm). After drying in air at 80°C for 4 h, the electrodes were pressed under 20 MPa for 1 min and then dried at 120°C for 24 h in vacuum. The weight of active materials in the electrode sheet was about 10 mg cm<sup>-2</sup>. The cells were assembled in an Ar-filled glove box. The electrolyte was 1 M  $\text{LiPF}_6$  in the mixture of ethylene carbonate and dimethyl carbonate with mass ratio being 1:1. A polypropylene film (Cellgard 2300) was used as the separator. The galvanostatic charge–discharge tests were conducted on a PCBT-138-8D-A battery program-control test system at 0.1–0.5 C rates (a nominal specific capacity of 120 mAh g<sup>-1</sup> was assumed to convert the current density into C rate) in the voltage range of 3.20–4.35 V (vs Li/Li<sup>+</sup>). The cyclic voltammogram (CV) tests

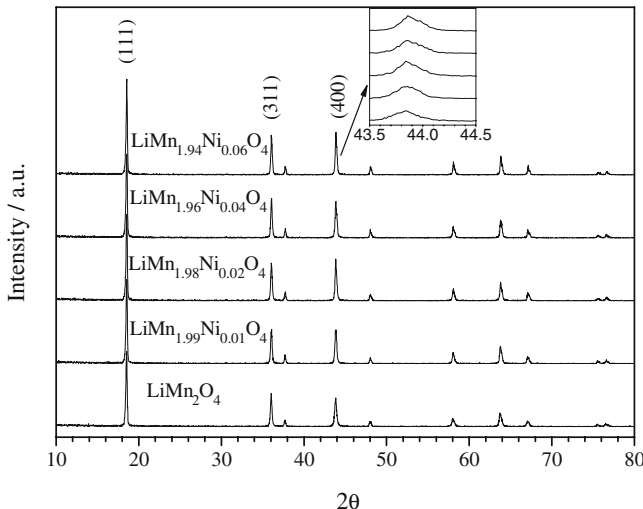


**Fig. 1** XRD patterns of Ni-substituted lithium manganese oxide  $\text{LiMn}_{2-x}\text{Ni}_x\text{O}_4$  with  $x=0.01, 0.02, 0.04, \text{ and } 0.06$

**Table 1** The lattice parameters and unit cell volume for Ni-substituted lithium manganese oxide  $\text{LiMn}_{2-x}\text{Ni}_x\text{O}_4$  with  $x=0.01, 0.02, 0.04, \text{ and } 0.06$

| Sample   | Lattice parameter (Å) | Unit cell volume (Å <sup>3</sup> ) |
|--|-----------------------|------------------------------------|
| $\text{LiMn}_2\text{O}_4$                      | 8.2440                | 560.29                             |
| $\text{LiMn}_{1.99}\text{Ni}_{0.01}\text{O}_4$ | 8.2406                | 559.59                             |
| $\text{LiMn}_{1.98}\text{Ni}_{0.02}\text{O}_4$ | 8.2386                | 559.19                             |
| $\text{LiMn}_{1.96}\text{Ni}_{0.04}\text{O}_4$ | 8.2353                | 558.52                             |
| $\text{LiMn}_{1.94}\text{Ni}_{0.06}\text{O}_4$ | 8.2343                | 558.31                             |

were performed on a CHI660A electrochemical workstation at room temperature with a scan rate of 0.1 mV s<sup>-1</sup>.

## Results and discussion

Figure 1 shows XRD patterns of undoped and Ni-doped  $\text{LiMn}_2\text{O}_4$  powders. The diffraction patterns of all the samples can be identified as an ordered spinel structure with space group Fd3m. There is no significant difference in the crystal structure after the doping. This indicates that the Mn site in  $\text{LiMn}_2\text{O}_4$  is substituted fully by Ni, and no other phase is formed. However, from the insert in Fig. 1, it is seen that the Bragg diffraction peaks go to the higher angle slightly with the increase in the amount of nickel. The lattice parameters and unit cell volumes of the samples are calculated from the XRD data and are recorded in Table 1. For the pure  $\text{LiMn}_2\text{O}_4$ , the lattice parameter and unit cell

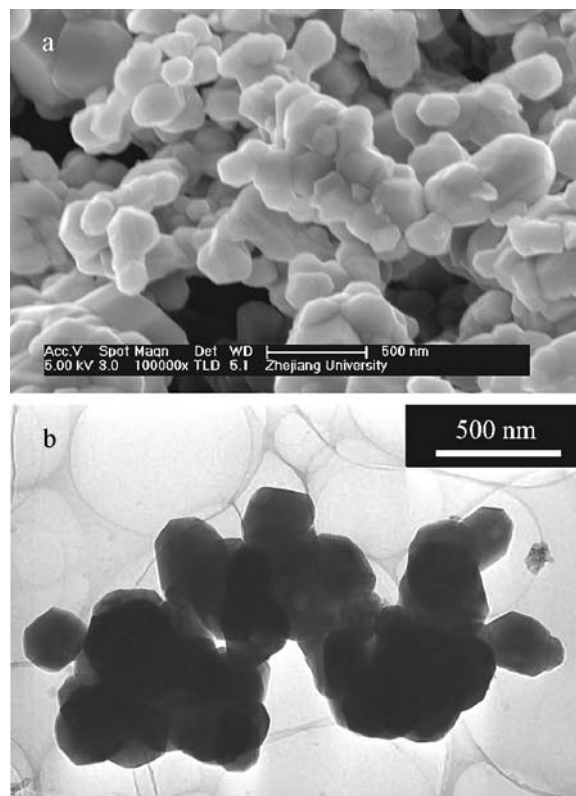


**Fig. 2** **a** SEM and **b** TEM images of  $\text{LiMn}_{1.98}\text{Ni}_{0.02}\text{O}_4$  powder

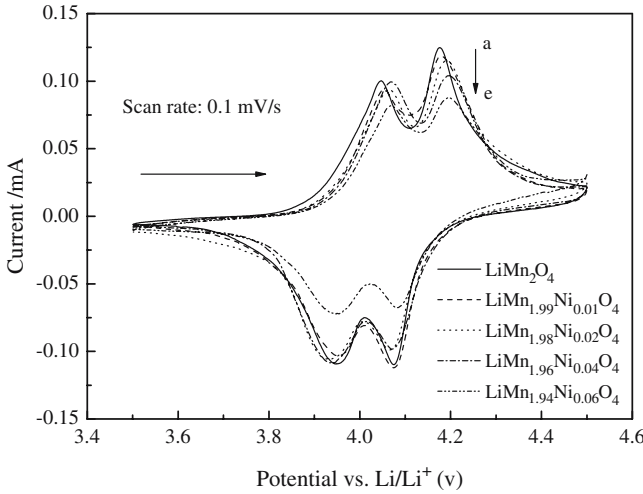


**Fig. 3** CV of as-prepared powders at a scan rate of  $0.1 \text{ mV s}^{-1}$ :  $\text{LiMn}_2\text{O}_4$ ,  $\text{LiMn}_{1.99}\text{Ni}_{0.01}\text{O}_4$ ,  $\text{LiMn}_{1.98}\text{Ni}_{0.02}\text{O}_4$ ,  $\text{LiMn}_{1.96}\text{Ni}_{0.04}\text{O}_4$ , and  $\text{LiMn}_{1.94}\text{Ni}_{0.06}\text{O}_4$

volume are  $a=8.2440 \text{ \AA}$  and  $V=560.29 \text{ \AA}^3$ . With the increase in the amount of nickel, the lattice parameter decreases gradually. According to the literature [15], this decrease is due to the increase in the concentration of  $\text{Mn}^{4+}$  ions in the spinel structure as  $\text{Mn}^{3+}$  ions are substituted by  $\text{Ni}^{2+}$  ions.

All the samples were synthesized under the same processing conditions as described in the experimental section by only changing the very minor stoichiometric compositions of the corresponding starting materials. All the as-prepared particles exhibit the similar submicro morphology. Figure 2 shows SEM and TEM images of  $\text{LiMn}_{1.98}\text{Ni}_{0.02}\text{O}_4$  powders. These images exhibit typical morphologies for all the as-prepared powders. The particles have an average size of about 200–300 nm and show uniform particle size distribution, but, from both images, it is obviously seen that the conglomeration takes place among the particles. In the

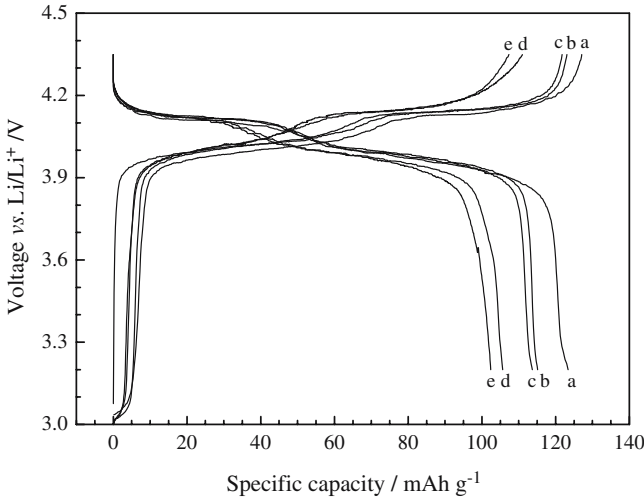


**Fig. 4** Initial charge/discharge curves of as-prepared powders at current density of  $0.1 \text{ C}$ :  $\text{LiMn}_2\text{O}_4$ ,  $\text{LiMn}_{1.99}\text{Ni}_{0.01}\text{O}_4$ ,  $\text{LiMn}_{1.98}\text{Ni}_{0.02}\text{O}_4$ ,  $\text{LiMn}_{1.96}\text{Ni}_{0.04}\text{O}_4$ , and  $\text{LiMn}_{1.94}\text{Ni}_{0.06}\text{O}_4$

TEM image (Fig. 2b), interference fringes are observed on fine particles. This suggests that the products are in a good crystalline state.

To evaluate the electrochemical characteristics of the as-prepared powders with the amount of doping Ni ion, a series of electrochemical tests was performed. Figure 3 shows the CVs of the powders between 3.5 and 4.5 V at a scan rate of  $0.1 \text{ mV s}^{-1}$ . The figures of five samples all present two pairs of peaks at 4-V region, which represents two redox reactions for undoped and doped  $\text{LiMn}_2\text{O}_4$ . Generally, these anodic and cathodic peaks on the voltammograms are related to the  $\text{Mn}^{4+}/\text{Mn}^{3+}$  couple. Thus, when the  $\text{Ni}^{2+}$  replaces  $\text{Mn}^{3+}$  site partly, the amount of redox  $\text{Mn}^{4+}/\text{Mn}^{3+}$  couple decreases. In Fig. 3, the difference among the five samples is that the two peak splits weaken with the increase in the amounts of Ni ion; the peaks become broader and shift toward higher potential than that of pure spinel  $\text{LiMn}_2\text{O}_4$ . The anodic and cathodic peaks on the voltammograms are related to the intercalation and deintercalation of lithium ions into and from the spinel. It is concluded that all samples displayed the typical two-step reversible lithiation/delithiation process of lithium ions in these solid powders, and the differences suggest that the amount of Ni ion doped affects the ability of lithium ions removed from the host powders, and with increasing the Ni ion, the ability decrease.

Initial charge and discharge curves of undoped and doped  $\text{LiMn}_2\text{O}_4$  are presented in Fig. 4. At a low current density ( $1/10 \text{ C}$ ) between 3.2 and 4.35 V, all the curves exhibit two clear charge and discharge flat plateaus approximately at 4 V, indicating that all the samples have a two-staged lithium insertion/deinsertion behavior, consistent with the cyclic voltammetry result. At these test voltage ranges, the initial discharge capacities of undoped  $\text{LiMn}_2\text{O}_4$  and doped  $\text{LiMn}_{2-x}\text{Ni}_x\text{O}_4$  ( $x=0.01, 0.02, 0.04, 0.06$ ) are  $123, 118, 116, 106, 102 \text{ mAh g}^{-1}$ , respectively. The specific capacity of samples decreases with the increase in the amount of Ni substitution. This phenomenon can be explained that the decrease in reversibly

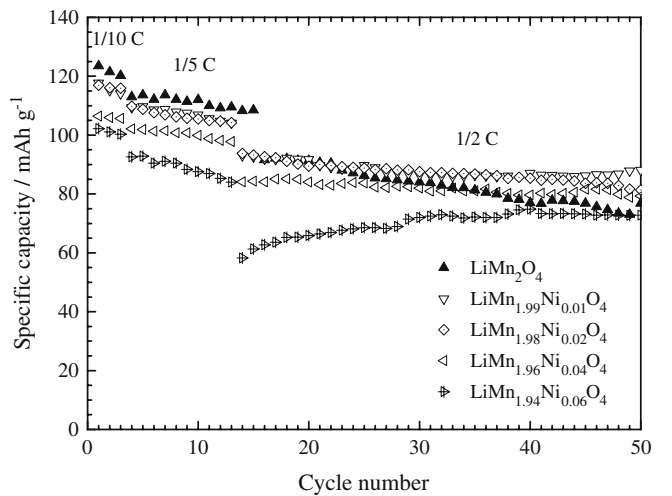


**Fig. 5** Discharge capacity vs cycle numbers for spinel  $\text{LiMn}_2\text{O}_4$  and doped  $\text{LiMn}_{2-x}\text{Ni}_x\text{O}_4$  ( $x=0.01, 0.02, 0.04$ , and  $0.06$ )

extractable Li ion amounts to “1” for undoped material  $\text{LiMn}_2\text{O}_4$  to “ $1-x$ ” for Ni substituted lithium manganese oxides upon electrochemically active  $\text{Mn}^{3+}$  ion substitution ( $\text{Mn}^{3+}$  content decrease,  $\text{Mn}^{3+}/\text{Mn}^{4+}$  corresponding to the potential of 4 V).

To study the influence of doping Ni ion on the cyclability, the cells were cycled as the following program: in the first three cycles, the current density was 1/10 C; in next ten cycles, it was cycled at 1/5 C, then using 1/2 C cycled to last. The results are shown in Fig. 5. For the undoped  $\text{LiMn}_2\text{O}_4$ , although it delivers a relatively high initial discharge capacity at low-current density, with increasing the current density, the capacity decreases a lot and fades very fast. On the contrary, with the increase in Ni doping, the initial capacity of  $\text{LiMn}_{2-x}\text{Ni}_x\text{O}_4$  delivers a slightly low discharge capacity. For  $\text{LiMn}_{1.96}\text{Ni}_{0.04}\text{O}_4$ , the capacity at 1/2 C was  $84 \text{ mAh g}^{-1}$ , but, after cycling, the capacity maintains above  $80 \text{ mAh g}^{-1}$ . Probably, due to the distortion of the unit cell during cycling, the capacity of undoped  $\text{LiMn}_2\text{O}_4$  decreased rapidly. Although Ni ions partly substitutes for manganese, they could effectively enhance the stability of the spinel structure, and furthermore, Ni ions do not get oxidized and reduced in the 3.2 to 4.35-V region, the result is a capacity reduction. It is surprising that in  $\text{LiMn}_{1.94}\text{Ni}_{0.06}\text{O}_4$ , the capacity decreases very largely when the current density increases, but, with increasing the cycle, the capacity increases.

## Conclusions

This study is focused on modifying the spinel  $\text{LiMn}_2\text{O}_4$ . Through a spray-drying method, undoped and doped  $\text{LiMn}_{2-x}\text{Ni}_x\text{O}_4$  materials were synthesized. Pure, single-

phase Ni-doped spinel  $\text{LiMn}_2\text{O}_4$  were obtained with very good crystallinity. The cyclic voltammetric experiments reveal that all the samples are good reversible about two-step lithiation/delithiation process. The initial undoped  $\text{LiMn}_2\text{O}_4$  and doped  $\text{LiMn}_{2-x}\text{Ni}_x\text{O}_4$  ( $x=0.01, 0.02, 0.04$ , and 0.06) were  $123, 118, 116, 106, 102 \text{ mAh g}^{-1}$ , respectively, but the cycle ability is significantly improved by the doping of  $\text{Ni}^{2+}$ . The spray-drying method will be an attractive method for fabrication of the spinel  $\text{LiMn}_{2-x}\text{Ni}_x\text{O}_4$  powders for lithium ion batteries.

---

## References

1. Tarascon JM, Wang E, Shokoohi FK, Mckinnon WR, Colson S (1991) J Electrochem Soc 138:2859
2. Sun YK, Yoon CS, Kim CK, Youn SG, Lee YS, Yoshio M, Oh IH (2001) J Mater Chem 11:2519
3. Tarascon JM, Guyomard D (1993) Electrochim Acta 38:1221
4. Pistoia G, Wang G, Wang C (1992) Solid State Ionics 58:285
5. Huang H, Bruce PG (1995) J Power Sources 54:52
6. Xia Y, Noguchi H, Yoshio M (1995) J Solid State Chem 119:216
7. Xia Y, Zhou H, Yoshio M (1997) J Electrochem Soc 144:2593
8. Yamada A, Tanaka M (1995) Mater Res Bull 30:715
9. Taniguchi I (2005) Mater Chem Phys 92:172
10. Kumar G, Schlorb H, Rahner D (2001) Mater Chem Phys 70:117
11. Yang ST, Jia JH, Ding L, Zhang MC (2003) Electrochim Acta 48:569
12. Thirunakaran R, Kim K-T, Kang Y-M, Seo C-Y, Jai Y-L (2004) J Power Sources 137:100
13. Dokko K, Mohamedi M, Anzue N, Itoh T, Uchida I (2002) J Mater Chem 12:3688
14. Bellitto C, DiMarco MG, Branford WR, Green MA, Neumann DA (2001) Solid State Ionics 140:77
15. Zhong Q, Bonakdarpour A, Zhang M, Gao Y, Dahn JR (1997) J Electrochem Soc 144:205